Physics Vol. 2, No. 5, pp. 221-245, 1966. Physics Publishing Co. Printed in Great Britain.

ISOTHERMAL FLOW OF LIQUID He II THROUGH NARROW CHANNELS*

W. E. KELLER and E. F. HAMMEL

Los Alamos Scientific Laboratory, University of California
Los Alamos, New Mexico

(*Received* 17 *November* 1965)

Abstract

Isothermal flow of liquid He II through narrow slits of width 0.3, 2.3, and 3.4 μ has been examined using two different types of experimental arrangements, one in which the liquid flows under its own gravitational head, the other in which the liquid is pushed by a plunger through the slit. In these experiments to a good approximation only the superfluid flows. Values of the superfluid critical velocity, $\mathbf{v}_s = \mathbf{v}_{s,c}$, *are found to be 18.0, 5.85, and 2.73 cm/sec for the three slits respectively, independent of temperature for the range* $1.1 < T < 2.0°K$. *At the λ point* $\mathbf{v}_{s,c}$ *becomes zero. At low temperatures, the critical velocities as obtained in these flows are the same as found in heat flow measurements using the same slits; but above 1.6°K results from the latter show that* $\mathbf{v}_{s,c}$ *increases. Possible reasons for this behavior are discussed in terms of the vortex line model, the principal conclusion being that for both isothermal flow and heat flow in narrow channels the breakdown of superfluidity occurs because of interactions between the superfluid and the wall. At supercritical velocities* ($\mathbf{v}_s > \mathbf{v}_{s,c}$) *the dissipation effects observed in isothermal flow can be described entirely in terms of a force* $\mathbf{F}_s$ *associated with the superfluid alone, whereas in the case of heat flow the mutual force* $\mathbf{F}_{sn}$ *is dominant. The present experiments show that the pressure gradient is proportional to* $\mathbf{F}_s$, *and* $\mathbf{F}_s$ *is independent of the slit width, has a temperature variation below 1.9°K much like that of the superfluid density squared, and depends upon the velocity as* $(\mathbf{v}_s - \mathbf{v}_{s,c})^n$. *For low supercritical velocities* $n = 1$ *and for* $(\mathbf{v}_s - \mathbf{v}_{s,c})$ *greater than about 1.5 cm/sec* $n = 1.75$. *These results are also considered from the viewpoint of the vortex line model.*

1. Introduction

EXPERIMENTS with liquid helium during the past twenty-five years have produced convincing evidence that below the λ point, under suitable conditions, the fluid may flow unaccompanied by energy dissipation, or in other words, exhibit superfluidity [1]. The characteristics of superfluidity and the mechanism for its destruction at some critical velocity have been extensively investigated both experimentally and theoretically; and although considerable progress has been made toward a description of superfluid hydrodynamics, a number of questions remain unresolved, particularly with regard to the flow processes in narrow channels.

* Work performed under the auspices of the U.S. Atomic Energy Commission.

While the distinction between "wide" and "narrow" channels has usually been somewhat arbitrary, there is an apparent division at $d \approx 10^{-3}$ cm, where d is the smallest dimension of the channel in a direction normal to the flow. For d greater than 10^{-3} cm (wide channels), the two-fluid model can be combined with the vortex-line model to give a reasonable description of some of the experimental results on He II flow, as for example, the variation of critical velocity with d [2]. However, for d less than about 10^{-3} cm (narrow channels) the predictions of the theoretical model begin to deviate from the observations and the discrepancies increase as d becomes smaller. It is indeed expected that the theory should break down, or at least require significant modification, when applied to such small dimensions that boundary effects become predominant. Furthermore, although this model primarily provides a physical interpretation of the interaction between the normal fluid and superfluid velocity fields through a so-called mutual force, it has never been altogether clear whether other forces may exist, e.g. a purely superfluid force, and if so, whether these too can be described by an extension of the model. The difficulties of the situation are compounded by a lack of consistency among the experimental results obtained for flows in narrow channels. This latter condition has provided the principal motivation for the investigations described in the present paper.

Specifically, the objectives of this work were: using narrow channels (a) to confirm, from data obtained in essentially isothermal flow experiments, the unambiguous existence of a superfluid critical velocity $\mathbf{v}_{s,c}$; (b) to investigate the dependence of $\mathbf{v}_{s,c}$ upon channel width and length and upon temperature; (c) to compare these values of $\mathbf{v}_{s,c}$ with those obtained from heat flow measurements [3]; (d) to investigate the manner in which superfluidity disappears as the λ point is approached from lower temperatures; (e) to determine whether the value of $\mathbf{v}_{s,c}$ depends on the magnitude and the sign of the fluid acceleration; and finally, but very importantly, (f) to establish the relationship between the pressure gradient and the superfluid velocity, $\mathbf{v}_s$, when $\mathbf{v}_s$ exceeds $\mathbf{v}_{s,c}$.

These objectives have been met by conducting isothermal flow experiments in two types of apparatus. In the first, the fluid is allowed to flow through the channel under its own hydrostatic head. In this type of flow, which we call gravitational flow (GF), the liquid is always decelerating and is always flowing supercritically, a small but finite extrapolation being necessary for a determination of $\mathbf{v}_{s,c}$. The second apparatus employs a plunger to force the liquid through the channel either at constant speeds, supercritical or subcritical, or under conditions of acceleration or deceleration. These flows we refer to as forced flows (FF). Both sets of experiments were run using the same channels through which heat flow and fountain pressure studies had previously been performed [3], so that the thermal and isothermal flow properties could be compared directly.

In the types of flow measurement under consideration the degree of uniformity of the channel may have a significant bearing upon the results and their interpretation, and it is quite possible that the inconsistencies between the many experimental data already reported for gravitational flow through narrow channels have in part been due to the use of poorly defined channels. Therefore, considerable effort was made in the heat flow experiments to construct and use slits with uniform, stable, and simple geometries which were readily measurable, and these advantages were transferred to the present work.

Although the gravitational flow of liquid He II has generally been considered equivalent to isothermal flow, it has been appreciated that, strictly speaking, this is not the case and that small differences in temperature develop between the ends of the channel during flow. These differences arise because primarily superfluid is transported through a narrow channel, so that the superfluid concentration is depleted at the entrance and enhanced at the exit. This process in turn produces a fountain pressure which is usually significant above 1.5°K (depending upon

the extent to which the apparatus is adiabatic), which is not effective in driving the fluid through the slit, and which must therefore be separated from the observed hydrostatic head. In previous work this effect has usually been neglected, and it is believed that this omission is another source of the inconsistencies mentioned earlier. Consequently, in the present work measurements of the temperature differences were made, and as expected, were essential for obtaining self-consistent results. Details of the corrections necessitated by these temperature differences are reported elsewhere [4].

2. Apparatus and Procedure

(a) Cryostats

Schematic drawings of the two types of apparatus are shown in Fig. 1, A being used for the FF experiments and B for the GF studies.

In A, the liquid is forced through the slit S by motion of the plunger P, which is a capped, thin-wall, nickel-alloy bellows; and the resultant pressure difference across the slit is indicated by the menisci levels in the glass standpipes H. The plunger is connected by a shaft (tubular in regions of large temperature gradients) to a driving system outside the cryostat. A frequency controlled synchronous motor, through a series of reduction gears, turns a precision-ground micrometer lead-screw in a close-fitting nut to which the plunger-rod is attached. The nut converts the screw rotation to a uniform translation of the plunger-rod. Motor speeds can be continuously varied in either direction from 500 to 5000 rev/min and any desired speed in this range can be held constant to 0.1 per cent. This system may be used to drive the liquid through the slit at a wide variety of constant velocities or in various accelerating or decelerating modes. Flow rates are determined from the rotational speed of the micrometer screw and from the geometry of the bellows and the slit. The volume of the bellows was calibrated at room temperature.

In these experiments the level differences associated with the various fluid velocities were measured using a cathetometer with an uncertainty equivalent to $\Delta P = 0.6$ dyn/cm^2. While the bellows was being driven a temperature difference was established across the slit, as discussed above; and when this effect was significant, the ΔT's were measured in order that the appropriate correction could be made.

The GF cryostat B consists of a closed system in contrast to the open bath system used in many previous similar experiments; and additional thermal isolation was achieved by placing a copper radiation shield (not shown in Fig. 1) around the glass walls G of the cell. A phenolic plunger P is manually operated from outside the cryostat and serves to adjust the initial level difference between the liquid inside (h_i) and outside (h_o) the glass standpipe H. In this way inflow and outflow measurements may be made, a cathetometer again being employed to measure the difference in liquid levels, $\Delta h = h_i - h_o$, as a function of time. The flow rate is obtained from the level observations plus a knowledge of the tube and slit dimensions. The corresponding pressure difference is given by Δh, corrected for ΔT effects and outside level changes.

Some runs with this apparatus were made with tube H sealed off at the top and others with the top open but narrowed down to a diameter of 0.045 cm. Two closed tubes were used having

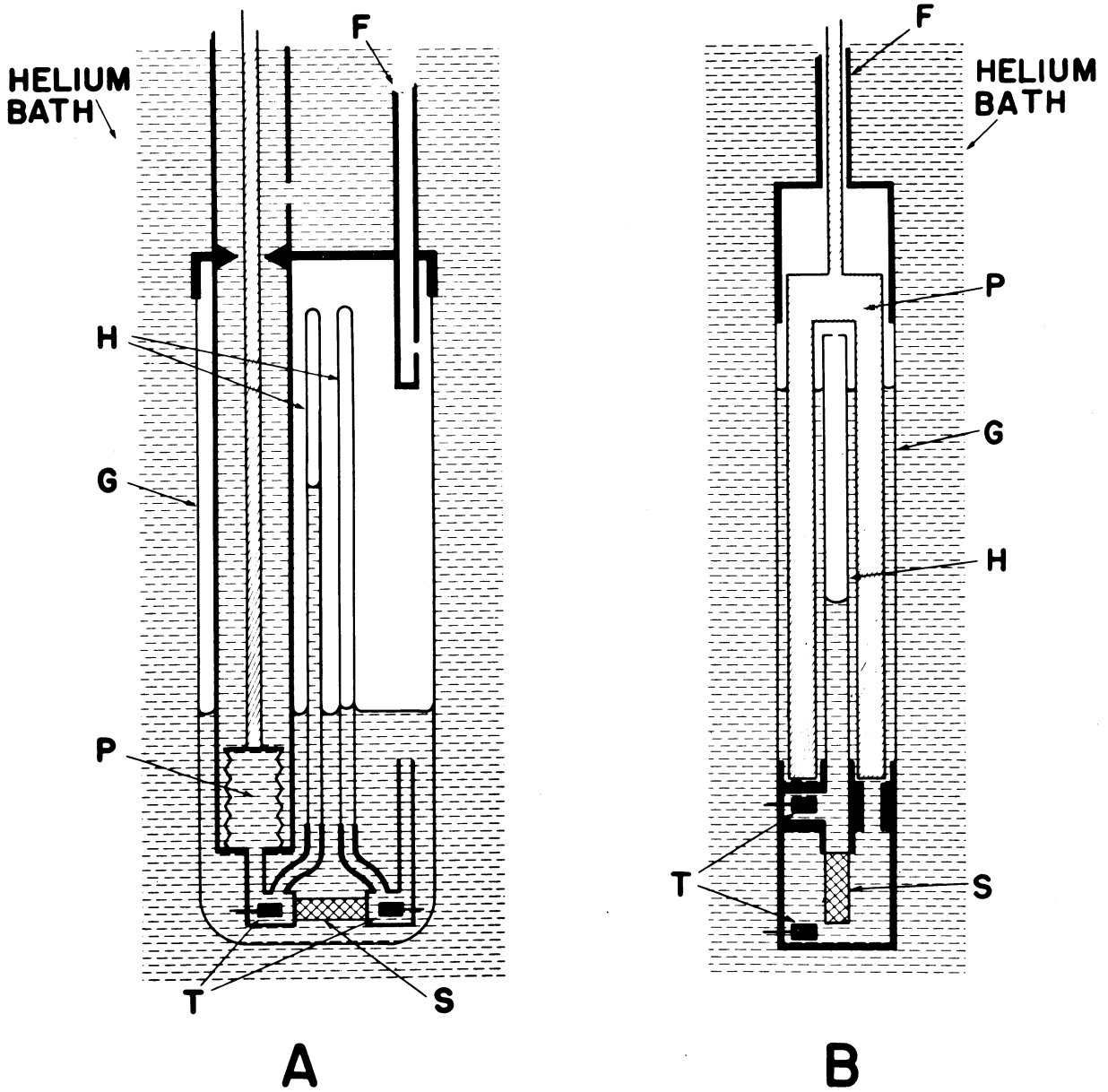

FIGURE 1

Two types of apparatus used for isothermal flow experiments, A for forced flow (FF), B for gravitational flow (GF); F, filling lines; G, glass walls of cells; H, glass standpipes; P, plungers; S, slits; T, carbon resistance thermometers.

inside diameters of 0.490 and 0.244 cm; the diameter of the open tube was 0.490 cm. For the open tube, corrections to the flow rate were made to account for the flow of the helium film.

The corrections, which were different for inflow and outflow, were determined experimentally and were at most less than 5 per cent of the total flow.

(b) Slits

The three channels used for these experiments have been fully described in a previous publication [3]. They are made from mating, hardened stainless steel cylinders and plugs such that the channel length is 1.9 cm and the breadth 1 cm. The width of the widest slit (Slit III′) was measured previously to be 3.36 μ. This slit was used in apparatus A without alteration and was the only slit studied in FF experiments. Slits I and II were the only basic slits used in apparatus B, and each of these was cleaned and lightly polished before use in the present experiment. This handling produced no more than a 10 per cent change in slit width in the channels.

After GF experiments were run with Slit I, the slit was altered in four successive steps which are illustrated in Fig. 2: (1) At section A-A′ of the plug, another "flat" was made (shown as heavy dotted line) without altering the centering features of this shoulder, but

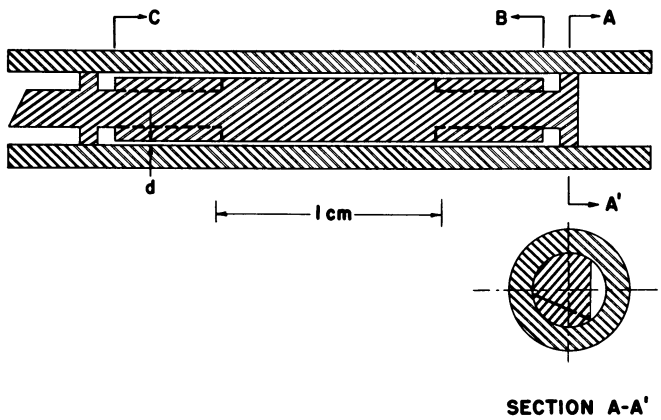

FIGURE 2

Slit geometry showing successive modifications as described in text.

enlarging the flow cross section. This change was made to ascertain whether this entrance (or exit) condition contributed to the flow results. (2) The sharp corner at position B was given a small radius, thereby altering the entrance of the slit proper; if end effects were important, such a change should affect the results. (3) The undercut at end B was enlarged, as shown by heavy dashed lines in the figure, in order to shorten the length of the slit by 25 per cent. (4) The undercut at end C was similarly enlarged to reduce the original length by 50 per cent. After each of the operations (3) and (4) the slit width was remeasured. Table 1 summarizes the pertinent information on the channels used.

TABLE 1

Slit geometries

Slit[a]	d (μ)	l (cm)	Remarks
I	2.29	1.90	Cleaned after use in heat flow experiments
I_1	2.29[b]	1.90	Additional flat on centering shoulder
I_2	2.29[b]	1.90	Corner at entrance rounded
I_3	2.64	1.44	Length reduced to ¾ that of original
I_4	2.70	0.965	Length reduced to ½ that of original
II	0.31	1.90	Cleaned after use in heat flow experiments
III′	3.36	1.90	Not cleaned after use in heat flow experiments

[a] All slits have breadth w = 1.0 cm.

[b] Slit width not measured, but assumed to be same as I.

(c) Meniscus Illumination

In the experiments described here an essential condition for obtaining reliable data is that the liquid menisci be clearly and uniformly illuminated over the whole range of observation. For measuring critical velocities it is necessary to distinguish very small level differences as well as to avoid confusion due to the presence of phantom menisci. Two effects combine to help isolate and identify the desired menisci: (1) the capillary rise due to surface tension in the standpipes; and (2) a small but constant difference in heat leak to the cells at opposite ends of the slit due to the asymmetric design – the accompanying fountain effect causes small reproducible displacements of the levels.

The range of level differences observed is up to about 70 mm. To illuminate uniformly the menisci over this range a fluorescent light and shutter arrangement, described elsewhere [5], was devised.

(d) Analysis of Data

The data for all the experiments described here have been analyzed under the assumption that the flow observed through the slits is due entirely to the superfluid component of the liquid helium and that, with the small pressure gradients and the narrow slits employed, any motion of

the normal component is too small to affect the results. Experimental justification for this assumption will be considered in a later section. The motion of the fluid may then be written as:

$$\rho_s \left(\frac{\partial \mathbf{v}_s}{\partial t} + \mathbf{v}_s \cdot \nabla \mathbf{v}_s \right) = - \frac{\rho_s}{\rho} \nabla P + \rho_s s \nabla T - \mathbf{F}_s - \mathbf{F}_{sn} \tag{1}$$

where $\mathbf{F}_s$, a generalized hypothecated superfluid force, may be considered a function of $\mathbf{v}_s$, $\mathbf{v}_{s,c}$, and T; and $\mathbf{F}_{sn}$, a generalized mutual force between the normal fluid and the superfluid, is usually taken to depend upon $(\mathbf{v}_s - \mathbf{v}_n)$, $\mathbf{v}_c$, and T; $\mathbf{v}_n$ is the normal fluid velocity, and $\mathbf{v}_c$ is some critical velocity, the exact specification of which is not yet clear. For the present experiments the left-hand side of (1) is effectively zero, so that by combining the two generalized forces into one, $\mathbf{F}_G$, and including in it the density dependence ρ/ρ_s, we find

$$- \frac{\rho}{\rho_s} \left[\mathbf{F}_s + \mathbf{F}_{sn} \right] = \mathbf{F}_G(\mathbf{v}_s, \mathbf{v}_n, \mathbf{v}_{s,c}, \mathbf{v}_c, T) = \nabla P - \rho s \nabla T \tag{2}$$

In this expression the independent variables are $\mathbf{v}_s$, $\mathbf{v}_n$, and T while $\mathbf{v}_{s,c}$ and $\mathbf{v}_c$ are considered as unknown parameters, characteristic of the liquid and dependent on T, for a given channel geometry.

Apparatus A was designed to explore the function $\mathbf{F}_G$ directly: with $\mathbf{v}_s$ and T being the independent variables ($\mathbf{v}_n = 0$), corresponding values of ∇P and ∇T are measured. The resultant driving force is plotted against $\mathbf{v}_s$ at various temperatures to give a convenient display of the data.

In apparatus B for GF, $\mathbf{v}_s$ is replaced by ∇P as an independent variable, allowing (2) to be considered from a different viewpoint. To determine $\mathbf{v}_s$, dh_i/dt must be obtained. It was found that for each experiment $h_i(t)$ could be accurately given by a polynomial. This expression is differentiated with respect to t and multiplied by the ratio of cross-section areas, giving the mean fluid velocity, $\bar{\mathbf{v}}$, through the slit. At this point, if the open tube is being used, the apparent velocity is corrected for film flow to obtain the true $\bar{\mathbf{v}}$. Then since

$$\begin{aligned} \rho \bar{\mathbf{v}} &= \rho_s \mathbf{v}_s + \rho_n \mathbf{v}_n \approx \rho_s \mathbf{v}_s, \\ \mathbf{v}_s &= (\rho/\rho_s) \bar{\mathbf{v}}; \end{aligned} \tag{3}$$

so that $\mathbf{v}_s$ represents the superfluid velocity averaged over the slit cross section. Values of $\mathbf{v}_{s,c}$ are obtained by solving the original polynomial for $t = t_e$ corresponding to the equilibrium position of h_i, i.e. that for which the gravitational head equals zero, and then determining the derivative at this point. These calculations were programmed for an electronic computer.

Data from the GF experiments when analyzed as described above showed always that $\mathbf{v}_s$ when plotted against ∇P approached $\nabla P = 0$ with a finite slope and at a finite intercept, thereby defining a critical velocity, $\mathbf{v}_{s,c}$ and imposing certain definite limits on the functional form of $\mathbf{F}_G$. It was considered desirable to confirm this behavior by a method of analysis independent of the polynomial form since the possibility exists that smoothing by the polynomial could force the results. Actually several different schemes were employed on randomly selected runs. For every case, the results of the analytical treatment were verified. It should be emphasized that not only were the values of $\mathbf{v}_{s,c}$ generally unaltered by these various analyses, but the character of the entire $\mathbf{v}_s$ vs. ∇P relation was unchanged as well.

3. Results

(a) Critical velocities

The results from both the FF and the GF experiments unambiguously demonstrate the existence of critical velocities associated with the superfluid motion in the geometries of the slits studied. Plots of v_s vs. ∇P for representative runs in apparatus B with Slits I and II are shown in Fig. 3. As discussed in the previous section, $v_{s,c}$ is easily identified from these data.

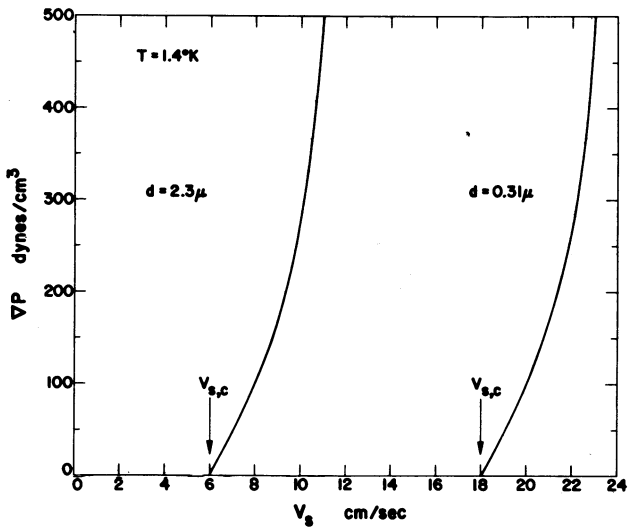

FIGURE 3

The pressure gradient ∇P as a function of superfluid velocity v_s observed in GF through two slits of different width d at the same temperature. The critical velocity in each case is indicated as $v_{s,c}$.

The temperature variation of $v_{s,c}$ for Slits I and II is plotted in Fig. 4, where the individual points are distinguished as representing either inflow or outflow measurements. Asymmetric conditions in the slit are seen to be not significant in these experiments. The values of $v_{s,c}$ remain constant over a large temperature range, strongly suggesting that for this range $v_{s,c}$ is independent of the amount of normal fluid present. While it might seem possible to extrapolate these results to lower temperatures, complete assurance to do this is lacking. (Kramers [6] has recently observed a temperature-independent $v_{s,c}$ in channels 100 μ wide down to 0.5°K; but we cannot rule out the appearance of some as yet unappreciated effect at still lower temperatures.) Our lack of understanding is made clear when we consider the rather unexpected results for $v_{s,c}$ in Slits I and II near the λ point. In both channels $v_{s,c}$ falls rapidly as T approaches T_λ, with the decrease starting at a lower temperature for the smaller slit. The dotted line in Fig. 4 is drawn to connect $v_{s,c} = 0$ at $T = T_\lambda$ with the average $v_{s,c}$ for the highest temperature runs of each slit (2.166°K for d = 2.29 μ and 2.151°K for d = 0.31 μ).

We consider now how the critical velocity changes with geometry. Several alterations were

made upon Slit I, as described above, and the various values of $v_{s,c}$ obtained at a temperature of 1.3°K are listed in Table 2. The temperature dependence of $v_{s,c}$ for Slits I_1 through I_4 is the same as for the original slit. It was expected that if the slit modifications were to affect $v_{s,c}$ in any way it would be in the direction of larger velocities. As seen from Table 2, the

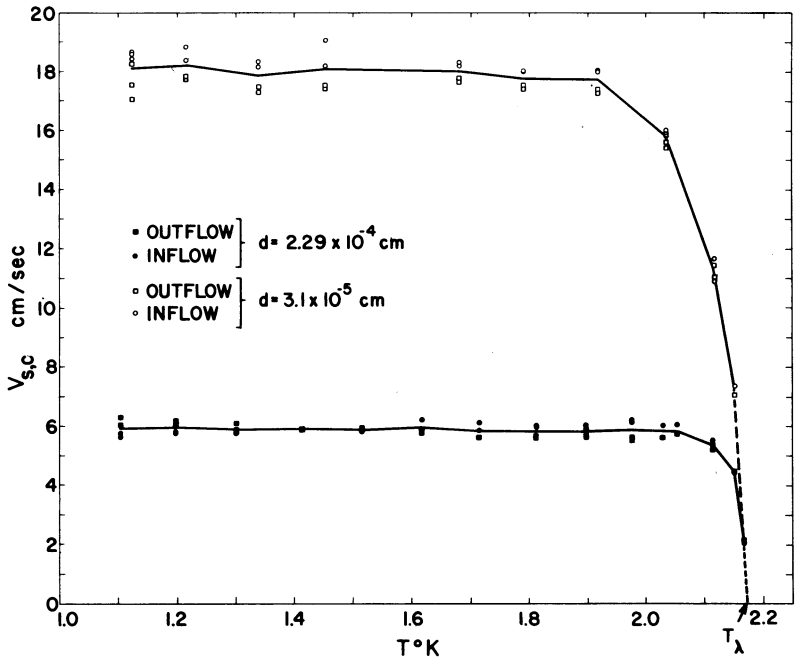

FIGURE 4

Critical superfluid velocities $v_{s,c}$ as a function of temperature T measured in GF for two slits of different width d. The solid lines connect the average values of $v_{s,c}$ at each T; the dotted lines are extrapolations to the λ point.

reverse was observed, $v_{s,c}$ decreasing somewhat from Slit I to Slit I_4. However, a compensation for this trend exists in that for the same progression, the slit width increases in a manner compatible with data on d vs. $v_{s,c}$ reported by previous workers [2]. With this taken into account, as well as our possible experimental errors, we deduce that had d been maintained constant $v_{s,c}$ would be relatively insensitive to changes in slit entrance (or exit) conditions as well as to a doubling of the slit length. At the same time we emphasize that the slit variations described here are not very drastic and that more work remains to be done before final conclusions can be drawn concerning the effect of slit length upon critical velocity.

Using Slit III′ in Apparatus A, an extensive series of FF experiments has also been carried out, covering the region from 1.05 to 2.11°K. The usefulness of this scheme for determining critical velocities consists in being able to establish steady subcritical flows at velocities right up to $v_{s,c}$. Figure 5 shows clearly a number of points at low v_s for which ∇P is zero within the uncertainty of establishing the liquid level positions. For velocities greater than $v_{s,c}$

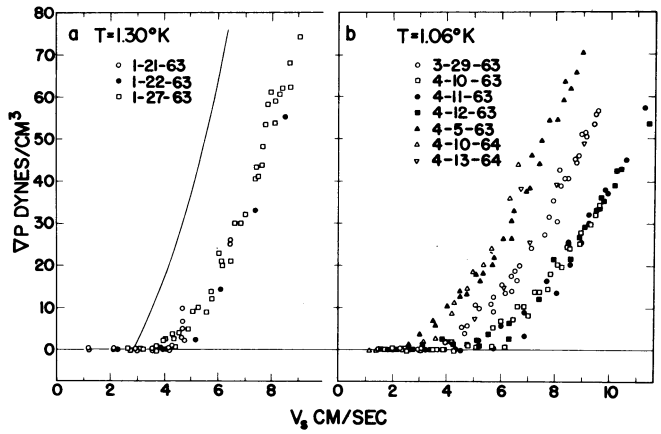

FIGURE 5

The pressure gradient ∇P as a function of superfluid velocity v_s observed in FF through Slit III′, d = 3.36 μ. The solid line in a represents the results of GF through the same slit.

the pressure gradient rises abruptly, as in the plots for GF. However, it has been much more difficult to obtain consistent values of $v_{s,c}$ from the FF than from the GF experiments. The exact reasons for this are not very well understood, but in practice we have often observed what might best be called "metastable" flows. By this we mean that if we take $v_{s,c}$ as determined by GF measurements to be the "condition of stability", it is frequently possible in FF experiments to exceed this value of $v_{s,c}$ by as much as a factor of two and to maintain this flow for several minutes before ∇P suddenly becomes different from zero. In these cases a ∇P vs. v_s curve is obtained which lies below that obtained from GF measurements, as illustrated in Fig. 5a. Furthermore, on separate days it often happens that different values of $v_{s,c}$ are produced with corresponding different dissipation curves. Frequently, the results for a new series of points would randomly and unaccountably alternate between two previously measured curves as the velocity was successively increased.

In order to establish the "condition of stability" for Slit III′ the standpipes of Apparatus A were altered to make possible GF and FF measurements in the same arrangement. The original standpipes had an inside diameter of 0.06 cm – a diameter which was deliberately chosen to be small in order to provide a sensitive means of observing fluctuations in level height, but too small to allow the level to be followed accurately once the plunger was stopped. These were replaced by standpipes with i.d. = 0.277 cm, in which small fluctuations were damped out. Measurements consisted of creating a head of some 6 cm of liquid He by rapidly moving the plunger, then stopping the plunger and observing the relaxation to $\nabla P = 0$. Results of eight such GF observations at 1.43 and 1.87°K gave a value of $v_{s,c} = 2.73 \pm 0.30$ cm/sec. The accuracy of these is less than that for results with Apparatus A since the level drop in B was considerably faster than in A. A typical ∇P vs. v_s plot of GF flow in A is given in Fig. 5a. In every case considered $v_{s,c}$ obtained from FF was equal to or greater than the corresponding results for GF within the accuracy quoted above. And as seen from Fig. 5b, flows with zero dissipation can be made to occur at velocities as high as 6 cm/sec in Slit III′.

TABLE 2

Average values of $v_{s,c}$, β, and γ obtained for Slit II and Various Modifications of Slit I at 1.3°K

Slit	$v_{s,c}$ (cm/sec)	β(g/cm^3 − sec)	γ(g/cm$^{3.75}$sec$^{0.25}$)
I	5.86 (4)[a]	38.0	32.2
I_1	5.33 (4)	39.0	34.4
I_2	5.05 (6)	31.0	26.0
I_3	4.04 (4)	44.1	36.8
I_4	3.96 (4)	39.9	31.6
II	17.83 (3)	35.8	28.5

[a] Number in parentheses indicates the number of experiments used in obtaining average values.

Many unsuccessful attempts were made to find correlations between these metastable observations and various external parameters of the system, such as vibration, temperature history, times for which the system remained quiescent, and other operating procedures. It also seemed possible that the drive mechanism could be responsible for creating spurious effects, either by supplying erratic impulses to the liquid through nonuniform motion of the bellows, or by giving erroneous velocity indications. Over a period of about a year radical changes and considerable refinements were made in the drive system, the final version being the one described earlier in this paper. As can be seen from Fig. 5b where results are shown for experiments spanning the period during which the modifications were made, improvements in the drive mechanism had virtually no effect upon the final numbers. From all of these experiences we can only conclude that in these metastable flows we are observing a perverse but true property of liquid helium and not an experimental artifact.

(b) Pressure Dependence of v_s

The similarities in the ∇P vs. v_s relationship suggested by Figs. 3 and 5 for the isothermal flows studied here are emphasized when the data are replotted as $\log(v_s - v_{s,c})$ vs. $\log \nabla P$. Figure 6 shows such a plot for several experimental runs at 1.3°K, each set of points representing data obtained from one of five different slit geometries. It is clear that despite these differences in slit configuration – which include changes in width over a range of almost ten as well as a variation in length by a factor of two – all the points fall remarkably close to a single curve. It is also evident that the flow through these slits exhibits at least three distinct regimes:

I. For velocities less than $v_{s,c}$, the superfluid flows frictionlessly and $\nabla P = 0$.

II. For superfluid velocities just above $v_{s,c}$, the points are on a curve with a slope of unity, which implies that $\nabla P = \beta(v_s - v_{s,c})$, where β is a constant.

III. At higher velocities the points fall along a line with slope of 4/7, indicating that here $\nabla P = \gamma(v_s - v_{s,c})^{1.75}$, where γ is another constant. The transition from region II to region III is not sharp, but the lines, when extrapolated, intersect at a value of $(v_s - v_{s,c})$ which may be designated as $v'_{s,c}$. Here $v'_{s,c}$ is equal to 1.65 cm/sec, and the corresponding ∇P is somewhat less than 100 dyn/cm^3. The measurement of pressure gradients in these experiments extends up to about 1000 dyn/cm^3, and at this limit the results are still characteristic of regime III.

In Table 2 the average values of β and γ are given for six different slit configurations at the same temperature. β has been determined at $\nabla P \cong 7$ dyn/cm^3 and γ at $\nabla P \cong 400$ dyn/cm^3. Within experimental error the numerical values of β and γ are effectively constant with the various slit modifications for a given temperature.

If we now consider how the pressure dependence varies with temperature, it is found that all the data – even for those runs near T_λ where the value of $v_{s,c}$ is appreciably reduced – can be represented on a single graph such as Fig. 6, but β and γ are functions of the temperature. This

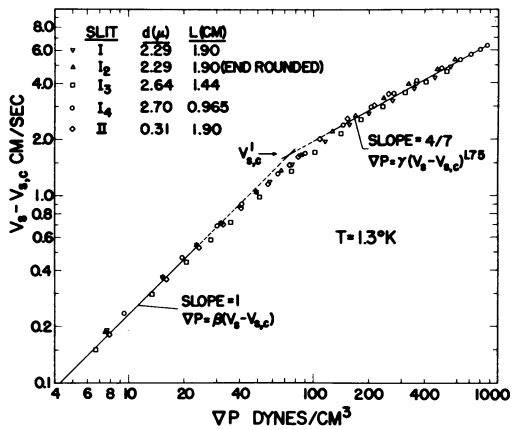

FIGURE 6

$(v_s - v_{s,c})$ vs. ∇P measured for GF through five different slit configurations at a single temperature.

dependence is shown in Fig. 7, where average values of β and γ are plotted for Slits I and II. Clearly, β and γ at a given temperature are the same for both slits throughout the range investigated. In addition, the temperature dependence of these two parameters is quite parallel as indicated by the solid lines in the figure. Finally, we should mention that the values of $v'_{s,c}$ for all the data fall between 1 and 2 cm/sec.

Turning now to the forced flow experiments, we describe first some additional details of the apparently capricious behavior mentioned earlier in connection with the critical velocities. It should be appreciated that a given point on one of the FF curves, such as shown in Fig. 5, may be obtained in a variety of ways, depending on the programming sequence of the drive motor.

Virtually all conceivable variations have been tried repeatedly and in no case has a significant correlation been found between the method used to excite the liquid and the resulting dissipation observed. For some temperatures, such as 1.30°K as shown in Fig. 5a, a single curve was always obtained, no matter what mode of fluid drive was used. Unaccountably, for other temperatures multiple results were obtained, but the multiplicity bore no relation whatever to the drive-motor programming. Nevertheless, in Fig. 5b we see three distinct, and perhaps four, dissipation curves, each of which has been reproduced on separate days. (Tests to determine whether various liquid heights in the cell affected the results were negative.)

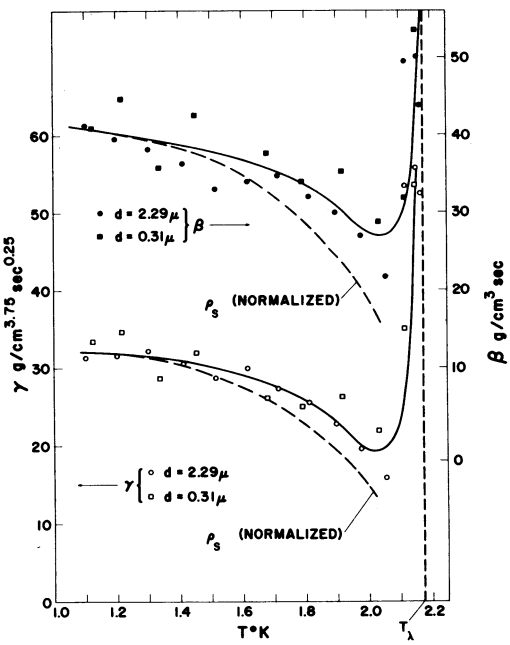

FIGURE 7

Average values of the parameters β and γ as a function of temperature. The solid lines represent smoothed curves through the data; the dotted lines give the temperature dependence of the superfluid density ρ_s normalized to the values of β and γ at 1.1°K.

It is clear from the scatter of the data that the results in detail cannot be treated as quantitatively as those for gravitational flow, although there is abundant indication that the dissipation curves are qualitatively similar. For the FF curves the two different flow regimes (n = 1 and n = 1.75) can in most cases be distinguished and values of β and γ obtained. Although the latter constants were generally not consistent with the results from GF in narrower slits, in three separate instances they were. Two of these occurred when FF and GF experiments with the wider standpipes were compared in the same apparatus at 1.43 and 1.87°K, and the third example was at the highest temperature, 2.11°K, using the narrow standpipes. For those cases where multiple ∇P vs. $\mathbf{v}_s$ relations are observed at a given temperature, such as shown in Fig. 5b, a distinct trend in the values of β and γ is noticeable. Proceeding from the lowest lying curve, having the largest apparent critical velocity and the minimum dissipation once that critical velocity is exceeded, toward that defined by the "stability conditions" in GF, the slopes

become steeper and thus β and γ increase. Thus the results for β and γ given in Fig. 7 appear to be an upper limit for the values of these parameters obtained in FF.

In all of the above analyses we have made the following two assumptions: (1) the irreversible loss of pressure gradient due to end effects is negligible; and (2) only superfluid contributes to the observed flow rates. The first assumption is clearly verified by the observation of lossless flow.

Considering the second assumption, we have observed the equivalent of 100 per cent normal fluid flow during the determination of d for Slit I using He I flow at 2.4°K. Assuming that the normal fluid flow below T_λ is governed by Poiseuille's law, it is easy to show that in the most unfavorable case – Slit I, $T > 2.1$°K, largest ∇P – the contribution by the normal fluid to the total flow is of the order of 2 per cent. For other instances this contribution is considerably less.

4. Discussion

Much of the following discussion of our results for narrow channels will be based on concepts of the quantized vortex-line model introduced by Onsager, Feynman, Hall and Vinen [7] even though the theory, especially as developed by the latter two authors, is expected to apply only to large geometries ($d > 10^{-3}$ cm). In spite of the fact that there have been repeated warnings of the additional complexities due to wall effects which might considerably alter the results for small geometries, the good description the theory gives of the heat flow experiments [8] in our narrow slits encourages us to continue to pursue the method of this model.

It must be admitted at the outset that the present results for $\mathbf{v}_{s,c}$, just as those of previous workers, do not conform in magnitude to the values predicted by the vortex-line model for $d < 10^{-3}$ cm. In the analysis which follows however it will be assumed that superfluidity is destroyed through the generation of vorticity in the superfluid fraction of the liquid; and although the physical situation is admittedly much more complicated, for the purposes of calculation it will be assumed that the form of vorticity most easily created is a ring-shaped line with roughly the diameter d of the channel. The properties of this ring are considered analogous to those of a classical vortex ring, with the exception that the circulation κ is quantized in units of h/m, m being the mass of the helium atom. Thus the superfluid velocity required to create a ring with radius $R = d/2$ and with one quantum of circulation is taken to be the critical velocity and is given by [9]

$$\mathbf{v}_{s,c} = \frac{\hbar}{md}\left[\ln \frac{4d}{a_0} - \frac{1}{4}\right] \tag{4}$$

where a_0, the core radius of the vortex, is thought to be of atomic dimensions, and may vary with the experimental conditions. Values of $\mathbf{v}_{s,c}$ for Slits I and II are calculated from (4) using $a_0 = 4$ Å to be 11.4 and 64.2 cm/sec respectively compared with the observed values of 5.85 and 18.0 cm/sec. Clearly, (4) predicts results which become progressively higher as d decreases. This is also seen in Fig. 8 where $\log \mathbf{v}_{s,c}d$ from a variety of different types of experimental data measured at 1.4°K is compared with the corresponding quantity obtained from (4). In this representation the values given by (4) have been multiplied by a factor of four in order to normalize the theoretical predictions to the experimental results for $d > 10^{-3}$ cm. There have been numerous attempts to bring the theory more in line with the experiments for $d < 10^{-3}$ cm, but none as yet has been successful. Peshkov [10] has given an empirical relation, in terms of

the vortex ring properties plus two additional arbitrary parameters, which fits the data shown in Fig. 8 over eight decades of d; but the physical basis for his treatment is not altogether satisfactory.

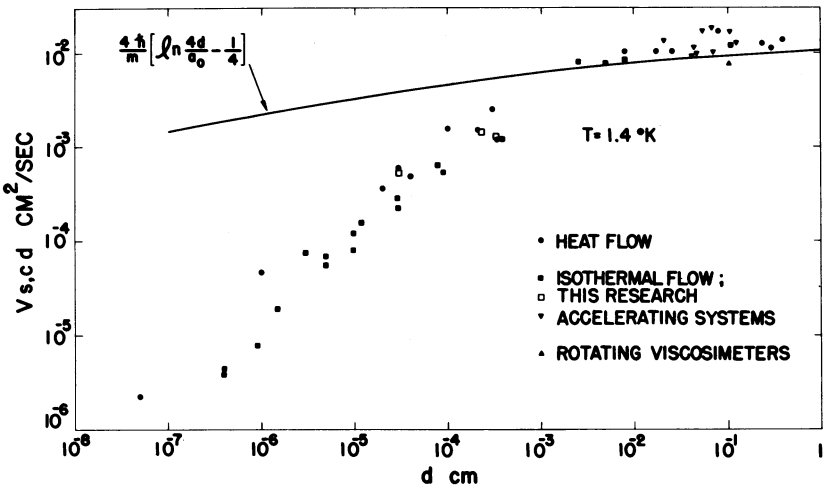

FIGURE 8

Comparison of the theoretical prediction of the channel-width dependence of $\mathbf{v}_{s,c}$ with values obtained from several different types of experiment. The solid line representing the theory is four times the quantity given by (4).

On the other hand, it is not certain that the experimental data with which (4) is being compared are wholly correct. As seen from Fig. 8, the present results for $\mathbf{v}_{s,c}$, while in reasonable agreement with those of previous workers, show a slightly different slope. Since these extend over only one decade in d, it is not possible to tell whether this difference is significant. Equation (4), however, does indicate that $\mathbf{v}_{s,c}$ should be independent of temperature and this is confirmed by the data presented in Fig. 4, except for the region near the λ point. In the past there has been little agreement on the temperature dependence of $\mathbf{v}_{s,c}$ as determined experimentally.

A qualitative explanation for the drop in $\mathbf{v}_{s,c}$ near the λ point is found in the Ginzburg and Pitaevsky [11] vortex-line model in which an order parameter ψ is considered equivalent to the superfluid wave function with the property that $|\psi|^2 = \rho_s$ at every point in the liquid. Near the walls of the container $\psi \to 0$ which implies that superfluidity occurs not because of the absence of a fluid-wall interaction but because ρ_s is zero at the walls. Also in the vicinity of a vortex core $\psi \to 0$ with decreasing r, so that near the core the value of ρ_s is quite different from its equilibrium value in the bulk liquid. From an investigation of the free energy of the liquid near T_λ and its dependence upon the spatial distribution of ρ_s, Ginzburg and Pitaevsky find that for a line with one quantum of circulation the "core" radius itself becomes very large, approaching infinity at T_λ according to the relation $a_0 \approx 4 \times 10^{-8}/(T_\lambda - T)^{\frac{1}{2}}$ cm. This analysis is appropriate only at temperatures near T_λ when a_0 is large compared to interatomic distances, i.e. $(T_\lambda - T) \lesssim 0.10$°K. Using this result for the temperature variation of a_0 together with (4) it is readily seen that $\mathbf{v}_{s,c}$ should go to zero at the λ point and that the

smaller the value of d the lower the temperature at which $v_{s,c}$ should begin to decrease, both effects conforming to the experimental results. A comparison of $v_{s,c}$ calculated from this a_0 dependence with $v_{s,c}$ observed in Slits I and II is given in Table 3. These calculated values of the critical velocity, $(v_{s,c})_{calc}$, are normalized to yield the observed temperature-independent critical velocity at low temperatures according to the expression

$$(v_{s,c})_{calc} = (v_{s,c})'_{calc} \times \frac{(v_{s,c})^{\circ}_{obs}}{(v_{s,c})^{\circ}_{calc}} \tag{5}$$

TABLE 3

Calculated critical velocities near the λ point

d (cm)	$(v_{s,c})^{\circ}_{obs}$ (cm/sec)	$(T_\lambda - T)$ (°K)	$(v_{s,c})_{obs}$ (cm/sec)	$(v_{s,c})_{calc}$ (cm/sec)
2.29×10^{-4}	5.85	0.056	5.37	4.81
		0.019	4.45	4.45
		0.010	2.12	4.18
3.1×10^{-5}	18.0	0.138	15.80	15.1
		0.057	11.3	13.9
		0.022	7.2	12.4

where $(v_{s,c})^{\circ}_{calc}$ is the limiting low temperature critical velocity given by (4) directly, $(v_{s,c})'_{calc}$ is the critical velocity calculated by (4) including the variation of a_0 with $(T_\lambda - T)$, and $(v_{s,c})^{\circ}_{obs}$ is the temperature-independent value observed in the experiments at temperatures below 2.0°K. The results for $(v_{s,c})_{calc}$ show the same trend as $(v_{s,c})_{obs}$, but are too high when $(T_\lambda - T)$ is small; it turns out that the agreement becomes much improved if $(T_\lambda - T)^{1/2}$ is replaced by $(T_\lambda - T)$. Considering the complexity of the actual situation, it is unreasonable to expect a better fit than this from such a simplified model. According to Ginzburg and Pitaevsky this variation in a_0 is also responsible for the lowering of the λ point observed in unsaturated films, as well as in very narrow channels ($d < 10^{-6}$ cm); any such effects as predicted by the theory would be much too small to be detected in the present experiments. It is of interest to point out the similarity between the temperature dependence of a_0 and that of λ, the London penetration depth of a magnetic field in a superconductor.

There has been some concern over how critical velocities should be defined in terms of experiments such as are reported here. In particular, Winen [7] has distinguished between "ideal" and "nonideal" critical velocities, depending on whether for $v_s < v_{s,c}$ the flow is exactly frictionless or just nearly so, and has pointed out the difficulties in determining which type

of flow is actually taking place in a given experiment. A further ambiguity exists when there are hysteresis effects accompanying the onset of frictional forces; thus the appearance of frictional forces as $\mathbf{v}_s$ is increased may occur at a higher velocity than that associated with the disappearance of these forces as $\mathbf{v}_s$ is decreased. Such effects were clearly seen in the measurements of heat flow in wide channels by Brewer and Edwards [12], who concluded that the lower value of $\mathbf{v}_s$ was the relevant one for determining the onset of nonlinear frictional effects due to interaction between the normal fluid and superfluid velocity fields. These heat flow data were characterized by large hysteresis effects which were markedly sensitive to mechanical vibration and considerably dependent upon previous history of the liquid. The magnitude of the hysteresis decreased with increasing temperature and disappeared near the λ point. The heat flow measurements performed through our narrow channels [3] never displayed hysteresis, whereas the isothermal forced flow data reported here seem to show a sort of metastable behavior in some respects similar to that observed by Brewer and Edwards. In the FF experiments the hysteresis appeared to be unrelated to either vibration or history, but it did diminish at higher temperatures. A distinction between heat flow and isothermal flow should be noted here; whereas in the former the critical velocity has been shown [8] to be associated with the onset of mutual friction, it will be seen that in the present isothermal flow experiments the dissipation apparently arises from superfluid forces alone. However, in agreement with the conclusion drawn from the Brewer and Edwards data, we also consider the lower value of $\mathbf{v}_{s,c}$ to be the significant quantity associated with the onset of frictional forces. In this respect the situation is quite analogous to that in classical fluids for the transition from laminar to turbulent flow. Here on acceleration, for a given fluid and given geometry, the critical velocity characterizing the transition may be considerably exceeded before instabilities in the flow occur; hysteresis is also observed, since on deceleration a lower critical velocity is obtained which is usually reproducible and is evidently determined by the decay processes of the turbulent eddies. For the case of pure superfluid flow the mechanism which we visualize as being responsible for the onset of friction involves the start of production of vorticity in the mainstream of the flow channel and this process may be quite unpredictable, depending upon particular circumstances of the experiment. It has been verified here, however, that $\mathbf{v}_{s,c}$ obtained in FF may be observed as low as but not lower than $\mathbf{v}_{s,c}$ for GF, so that under certain conditions the generation and decay of vorticity are equivalent processes. It therefore seems fairly clear that the lowest value of $\mathbf{v}_{s,c}$, being stable and reproducible, represents a fundamental property of the liquid.

The functional form of the force $\mathbf{F}_G$ of (2) is defined by the experimental ∇P vs. $\mathbf{v}_s$ curves, since all the data as presented have been corrected for the effect of the last term in this equation, $-\rho s \nabla T$. We recall that $\mathbf{F}_G$ was considered to be sufficiently general to include contributions from both mutual friction and superfluid friction. Since in the experiments $\mathbf{v}_n = 0$ and the relative velocity $\mathbf{v}_r = \mathbf{v}_s - \mathbf{v}_n = \mathbf{v}_s$, the $\mathbf{F}_{sn}$ term, should mutual friction be effective, would contribute to ∇P an amount of force unit volume given by

$$\frac{\rho}{\rho_s}\mathbf{F}_{sn} = A\rho\rho_n(\mathbf{v}_s - \mathbf{v}_c)^2\mathbf{v}_s \tag{6}$$

where A is an empirically determined function of temperature, probably independent of slit width [8] and $\mathbf{v}_c$ is some critical velocity. However, the quantitative analysis of the data for GF leaves absolutely no room for the appearance of mutual friction in the present experiments. The parameters entering equation (6) are sufficiently well known, and hence, if we put $\mathbf{v}_c = \mathbf{v}_{s,c}$, $\mathbf{F}_{sn}$ can be calculated. Such a calculation shows that at low temperatures, if mutual friction were present it would contribute so slightly to the dissipation that it could not be detected. At high temperatures, $\sim 2°K$, it would contribute significantly, and for Slit II, in fact, the

$\mathbf{F}_{sn}$ term would exceed by a considerable amount the total observed dissipation. In any event the $\mathbf{F}_{sn}$ contribution would lead to a much more temperature-dependent dissipation function than is found; furthermore, although some indication of a cubic dependence of $\mathbf{F}_G$ upon $\mathbf{v}_s$ should be expected, none has been found. We conclude therefore that for isothermal flow in narrow slits

$$\mathbf{F}_G = \frac{\rho}{\rho_s}\,\mathbf{F}_s = \frac{\rho}{\rho_s}\,\mathbf{F}_s\left[T, l, \left(\mathbf{v}_s - \mathbf{v}_{s,c}\right)\right], \tag{7}$$

noting that $\mathbf{F}_s$ is independent of d and of the actual value of $\mathbf{v}_{s,c}$.

We may arrive at a description of the dissipation process occurring in slits such as have been used in the present experiments following a line of reasoning suggested by Feynman [7], and developed further by Anderson [13]. If ψ_0 is the ground state wave function for the superfluid at rest, Feynman proposed that the form of the wave function Ψ for the fluid moving with a velocity $\mathbf{v}_s(\mathbf{r})$ should be given by

$$\psi = \psi_0 \exp\left(\frac{im}{\hbar}\sum_j \mathbf{v}_j(\mathbf{r}_j)\cdot\mathbf{r}_j\right) = \psi_0 \exp\left(i\sum_j \varphi(\mathbf{r}_j)\right)$$

where $\sum_j \varphi(\mathbf{r}_j)$ is the total phase.

Using this wave function the momentum current density $\mathbf{J}$ for superfluid helium can be shown to be

$$\mathbf{J} = \rho_s\mathbf{v}_s = (\hbar/m)\;\psi_0\psi_0^*\nabla\varphi \tag{8}$$

from which

$$\mathbf{v}_s = (\hbar/m)\;\nabla\varphi. \tag{9}$$

$\psi_0\psi_0^*$ is assumed† equal to ρ_s as discussed earlier in connection with the Ginzburg and Pitaevsky [11] calculation of a_0. The phase φ of the order parameter has been shown by Beliaev [14] to be proportional to the product of the chemical potential μ and the time; and as a consequence of the conjugaticity of φ and N, the number of superfluid quasi-particles, Anderson has obtained as one of the two Hamiltonian equations of motion the expression

$$\hbar\frac{d\varphi}{dt} = \frac{\partial E}{\partial N} = \mu,$$

which relates the conjugate variables φ and N (as well as E and t) to the chemical potential μ. If we now have a flow system such as used for the present experiments in which a narrow channel of length l connects two reservoirs I and II, and if we begin with $\mathbf{v}_s = 0$ through the channel and subsequently impose a constant $\nabla\mu$ such that $\mu_I > \mu_{II}$ (as for example, by adjusting the levels to make $H_I > H_{II}$) then the fluid will accelerate at a constant rate given by

$$\frac{d\mathbf{v}_s}{dt} = \frac{\hbar}{m}\frac{d}{dt}\nabla\varphi = \frac{\hbar}{m}\frac{d}{dt}\left(\frac{\varphi_{II} - \varphi_I}{l}\right) = \frac{1}{m}\left(\frac{\mu_I - \mu_{II}}{l}\right) \tag{10}$$

† Anderson [13] has pointed out that this identification cannot be justified except at $T = 0$, and terms (9) a "pseudo-identity".

until the critical velocity is reached. While the fluid is accelerating the relative phase of the fluid in reservoirs I and II is changing. If after a time t, the acceleration is stopped leaving the flow at some steady value of $\mathbf{v}_s < \mathbf{v}_{s,c}$ the level difference and hence $\Delta\mu$ vanishes and no additional phase change will be produced. From (9) however we will have

$$\mathbf{v}_s = \frac{\hbar}{m}\left(\frac{\varphi_{II} - \varphi_I}{l}\right) = 2\pi \frac{n}{l}\frac{\hbar}{m} = \frac{n\kappa}{l} \tag{11}$$

where n is the number of quanta of circulation generated during the acceleration period. †

Our model‡ is, then, that for steady subcritical flows there will exist along the channel walls a number n of vortex lines with axes aligned perpendicular to the flow; these lines will be stationary. Since the flow is steady no additional lines are being produced and the liquid flows without dissipation; furthermore, ideally the "lines" will be evenly distributed along the channel length. The situation is quite analogous to that of a bucket of He II rotating at an angular velocity ω; here the average vorticity is proportional to ω, and if ω is held constant, the number of vortex lines per unit area remains fixed. If now we increase $\mathbf{v}_s$ in the slit to some other steady rate with $\mathbf{v}_s > \mathbf{v}_{s,c}$, a constant $\Delta P = \rho g \Delta H$ is observed. Under these conditions $\nabla\mu$ is no longer zero indicating that circulation is being continuously produced and moving through the body of the fluid. In order to take into account this production another term must be added to the superfluid equation, namely the frictional term $\mathbf{F}_s$. Thus (10) becomes

$$\frac{d\mathbf{v}_s}{dt} = -\nabla\frac{\mu}{m} - \left(\frac{1}{\rho_s}\right)\mathbf{F}_s . \tag{12}$$

In the steady state the left-hand side of (12) equals zero, thereby giving a connection with (7). It is important to note that $\mathbf{F}_s$ in this case has been shown experimentally to be proportional to the pressure gradient, which means physically that the dissipation occurs equally along the entire length of the channel and not just at either end or at isolated spots along the length. In addition, the only condition upon the width of the channel, d, made in these arguments is the implied one that d be small enough to allow the approximation $\mathbf{v}_n = 0$, which in turn permits (12) above to describe the flow process. Confirmation of these conclusions is given in Fig. 6 where the experimental data for gravitational flow clearly illustrate the nature of the dependence of $\mathbf{F}_s$ upon length as well as the lack of dependence upon d.

The manner in which $\mathbf{F}_s$ is related to $(\mathbf{v}_s - \mathbf{v}_{s,c}) = \tilde{\mathbf{v}}$ admits of a physical interpretation also in terms of the above model. For $\mathbf{v}_s < \mathbf{v}_{s,c}$ we have potential flow, so that for all velocities up to $\mathbf{v}_{s,c}$ there should be no contribution to the dissipation function. The process of

---

† In this expression n need not be integral. As remarked later, any "circulation" probably occurs near the wall where $\Psi \simeq 0$ and is not of much physical importance.

‡ It is recognized that an arrangement of vortex lines such as is here postulated would be unstable classically except at a single subcritical velocity. Since quantized vorticity must be produced somewhere between I and II for finite subcritical flows, however, it is assumed that the essential elements of the calculations which follow will not be appreciably altered when an exact description of the dissipation process becomes available. Equally well, since at the walls $\psi_0 = 0$, we may think of the superfluid as simply slipping freely at the wall and not introduce the wall vorticity at all.

exceeding $\mathbf{v}_{s,c}$ is equivalent to passing from a one-dimensional flow (plane velocity profile to a two-dimensional one in which the plane velocity profile is modified by the introduction of vortex line segments into the mainstream. Experimentally it is found that

$$\nabla P = \beta \tilde{\mathbf{v}} = -\left(\frac{\rho}{\rho_s}\right) \mathbf{F}_s . \tag{13}$$

The linear dependence of $\mathbf{F}_s$ upon $\tilde{\mathbf{v}}$ seems reasonable since the flow of vorticity is initially not dense; hence interactions between adjacent vortices should be small and the dissipation should be of the lowest order analogous to laminar flow in ordinary fluids. The analogy with classical laminar flow cannot, however, be drawn much further, since the Poiseuille relation requires that β be proportional to d^{-2}, whereas it is observed in these experiments that β is independent of d. Thus it is not possible to define a superfluid viscosity in the usual sense. Another possible classical comparison might be made with boundary layer resistance which would be independent of d; but then the dissipation, i.e. ΔP, should depend upon $l^{1/2}$ or $l^{4/5}$ determined by whether the boundary layer were laminar or turbulent. The strict dependence of ΔP upon l discussed above rules out the boundary layer analogy.

In the vicinity of $\tilde{\mathbf{v}} = \mathbf{v}'_{s,c}$ there is an additional change in the flow pattern to one in which $\mathbf{F}_s$ is given by

$$\nabla P = \gamma(\tilde{\mathbf{v}})^{1.75} = -\left(\frac{\rho}{\rho_s}\right) \mathbf{F}_s . \tag{14}$$

This functional dependence upon velocity is once more reminiscent of a classical case, the transition from laminar to turbulent flow (Blasius rule). On this basis it is conjectured that at $\mathbf{v}'_{s,c}$ the orderly two-dimensional flow of vorticity described by (13) breaks down to the three-dimensional flow characteristic of turbulence. Since near $\mathbf{v}'_{s,c}$ the density of vorticity probably becomes appreciable, the possibility of interaction between neighboring vortices becomes considerably enhanced over what it is in the lower velocity regions and leads to a, higher order dissipation process. Further attempts to compare (14) with classical turbulence are not warranted.

In order to obtain some quantitative ideas concerning this model let us calculate ν, the rate of production of vorticity in the slit. The work done per second against friction on the fluid in the slit when $\mathbf{v}_s$ exceeds $\mathbf{v}_{s,c}$ will be called W_T; and this is equal to $\mathbf{v}_s \nabla P(lwd)$ ergs/sec (w is breadth of channel). In our description of the dissipation process we assume that W_T all goes to the production in the slit of vortex lines each with energy ϵ at a rate ν sec^{-1}. Thus

$$W_T = \mathbf{v}_s \nabla P\,(lwd) = \epsilon\nu. \tag{15}$$

We have no certain idea of what form the vortex lines would take, but it seems reasonable that the lines should have a characteristic or average length of the order d, either as rings or as lines stretched across the slit. In the former case, ϵ will be the energy to form a ring of diameter d and in the latter case will be the energy to create a line of length d; for either choice the results will be approximately the same, so we arbitrarily select the ring form. Then

$$\mathbf{v}_s \nabla P(lwd) = \nu\epsilon = \frac{\nu\rho_s \kappa^2 d}{4}\left[\ln \frac{4d}{a_0} - \frac{7}{4}\right],$$

or with $w = 1$ cm and the expression in the square brackets denoted by D, we obtain

$$\nabla P = \frac{\nu \rho_s \kappa^2 D}{4\, l \mathbf{v}_s}, \tag{16}$$

which is very nearly independent of d. From (13) and (16) we find

$$\nu = \frac{4\beta \tilde{\mathbf{v}}\, \mathbf{v}_s\, l}{\rho_s \kappa^2 D}. \tag{17}$$

showing that the rate of production of vorticity is proportional to both $\mathbf{v}_s$ and $(\mathbf{v}_s - \mathbf{v}_{s,c})$. Experimentally we observe that the temperature dependence of β is that of ρ_s from 1.1 to about 2.0°K. In Fig. 7 β is plotted vs. the temperature, and it is seen that below 2.0°K the agreement with the scaled values of ρ_s is quite reasonable.

Inserting the observed values of β into (17) one may calculate the frequency of formation of vortex rings in the channels, and from this the average spacing $\mathscr{L}$ of vorticity for various fluid velocities. We imagine that there might be some sort of competition between destruction and production of vorticity; but ν represents the net steady state rate of production for $\nabla P > 0$. Thus if $L_0 = \nu \pi d$ is the total length of line issuing from the channel/sec, the length of line L in the channel at any instant is $L_0 l/\mathbf{v}_s$, assuming that the vorticity moves at the same velocity as the superfluid. In particular we find that for $\tilde{\mathbf{v}} = 1$ cm/sec $\approx \mathbf{v}'_{s,c}$, $\nu \approx 2 \times 10^8$ rings/sec and $\mathscr{L} = L^{-\frac{1}{2}} \approx 1 \times 10^{-4}$ cm, of the order of the slit width. This conclusion adds substance to our conjecture that the mutual interaction of neighboring vortices is the origin of the transition near $\mathbf{v}'_{s,c}$.

We should like to return now to the various temperature dependences of $\mathbf{v}_{s,c}$ that have been observed experimentally. It usually has been assumed in making comparisons of $\mathbf{v}_{s,c}$, such as the one shown in Fig. 8, that $\mathbf{v}_{s,c}$ is essentially independent of the experimental method used for the determination. The data in Fig. 8 bear this out to a large extent. However, we wish to show in the following how differences do appear when this situation is examined in detail and how indeed observations of $\mathbf{v}_{s,c}$ by different methods are not necessarily equivalent.

The basis for discussion is the comparison of the $\mathbf{v}_{s,c}$ vs. T relation as obtained in the isothermal flow measurements described in the present work with this relation as determined previously using heat flow measurements in the same slits. In Fig. 9 such a comparison is made for Slits I and III′. The solid lines represent $\mathbf{v}_{s,c}$ determined from GF data. For Slit I these are taken as a smoothed curve from Fig. 4; and for Slit III′ the values of $\mathbf{v}_{s,c}$ are given with a spread, since the measurements are not so accurate as those for Slit I, for reasons described earlier. Solid circles in the figure are taken from Table 3 of [8] together with some intermediate unpublished values of the critical velocity. For clarity in the present discussion, $\mathbf{v}_{s,c}$ will continue to mean the GF results and $\mathbf{v}^*_{s,c}$ will be used to distinguish the heat flow critical velocities. It is seen from Fig. 9 that at low temperatures $\mathbf{v}_{s,c} = \mathbf{v}^*_{s,c}$, but beginning at ~ 1.9°K for Slit I and at ~ 1.6°K for Slit III′, $\mathbf{v}^*_{s,c} > \mathbf{v}_{s,c}$. Near the λ point it is seen that $\mathbf{v}^*_{s,c}$ rises while $\mathbf{v}_{s,c}$ falls rapidly to zero at T_λ. For wide channels, Peshkov and Strukov [15] have demonstrated that the onset of dissipation in both counterflow and pure superfluid flow is determined only by $\mathbf{v}_s$, just as indicated here for the results at low temperature and for narrow channels.

In order to recall how $\mathbf{v}^*_{s,c}$ has been determined we refer to Fig. 10 where P_f, the fountain

pressure, is plotted as a function of T for several reference temperatures T_0. Each curve represents the values of P_f observed across the slit when one end is held at T_0 and the other is

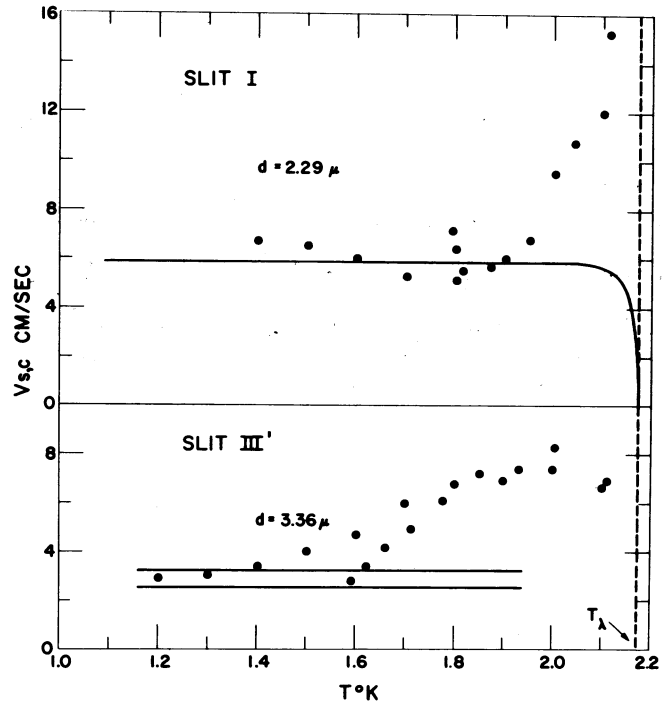

FIGURE 9

Comparison of the temperature variation of $\mathbf{v}_{s,c}$ as measured by isothermal flow (solid lines) and by heat flow (solid circles) in the same slits.

heated to successively higher equilibrium temperatures. Heavy solid lines in the figure represent the integrated ideal fountain pressure, and the point at which these lines depart from the experimental points defines $\mathbf{v}^*_{s,c}$ as determined by the known heat flow, $\bar{q}$, through the slit. Similar but independent measurements of $\bar{q}$ vs. T have been treated in the same manner, the results for $\mathbf{v}^*_{s,c}$ being in excellent agreement with values obtained from P_f vs. T. The break-away points such as shown in Fig. 10 are quite sharp and it is clear that for values of $\mathbf{v}_s < \mathbf{v}^*_{s,c}$ there is negligible dissipation in the fluid other than that due to ordinary viscosity of the normal fluid. Above $\mathbf{v}^*_{s,c}$ the observed curves are well explained by the appearance of a mutual friction force as given by (6) with $\mathbf{v}_s$ replaced by $\mathbf{v}_r = \mathbf{v}_s - \mathbf{v}_n$.

Thus at low temperatures for which $\mathbf{v}_{s,c} = \mathbf{v}^*_{s,c}$, the supercritical behavior of heat flow and of isothermal flow are distinguished in that the former is conventionally associated with mutual friction and the latter with superfluid friction alone. The criterion for an effective mutual friction, at least of the type considered by Vinen [16], is that the vorticity be homogeneously distributed in the liquid, or in other words, that the average spacing $\mathscr{L}$ between vortex lines be small compared with the slit width. This spacing may be estimated from Fig. 1 or equation (33)

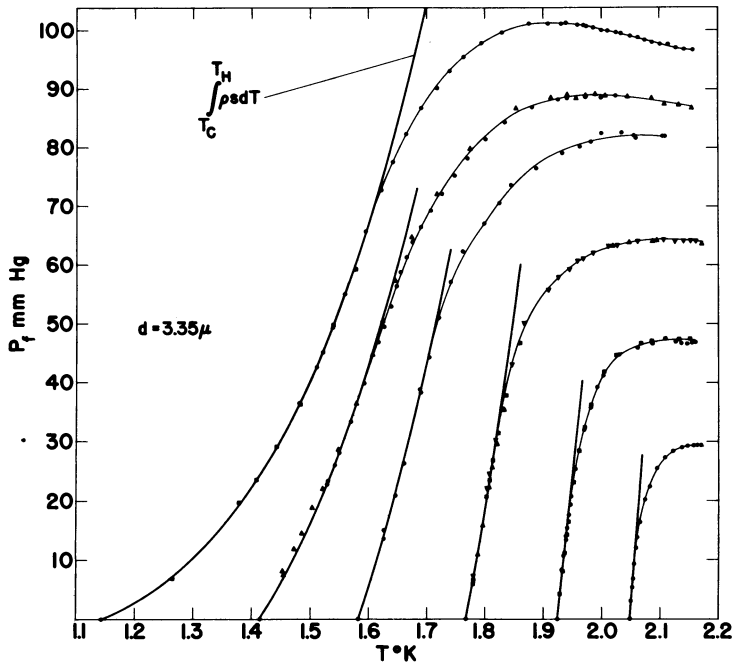

FIGURE 10

Integrated fountain pressure P_f vs. temperature obtained with Slit III' (d = 3.36 μ) for six different T_0's. Heavy solid curves are calculated from the London equation.

of [16] and is found to be inversely proportional to the relative velocity $\mathbf{v}_r$. Consider now the specific case of the curve in Fig. 10 beginning at T_0 = 1.15°K. At the breakaway point where $\mathbf{v}_s = \mathbf{v}_{s,c}^*$, $\mathbf{v}_r$ is of the order 100 cm/sec at the cold end, and $\mathscr{L} \approx 1 \times 10^{-4}$ cm. At slightly lower values of $\mathbf{v}_s$, $\mathbf{v}_r$ is still very large and hence $\mathscr{L}$, if it were formally calculated, would still be small. Thus even though the vortex lines if present could be considered homogeneously distributed, there is still no discernible indication of mutual friction. It is clear that before mutual friction can become operative, vorticity must first be produced in the channel; and this as we have seen can occur only for $\mathbf{v}_s = \mathbf{v}_{s,c}$. For the isothermal case corresponding to the heat flow example just mentioned, $\mathbf{v}_r = \mathbf{v}_s \approx 3.5$ cm/sec at the critical velocity, from which $\mathscr{L} \approx 3 \times 10^{-3}$, ten times larger than d. Here the criteria for the existence of a mutual friction force are not met and no such force is observed. From these considerations we conclude that for all temperatures when $\mathbf{v}_s = \mathbf{v}_{s,c}$ vorticity is created in the channel and for both types of flow this originates from interactions associated only with the superfluid. Hence (1) no matter how large $\mathbf{v}_r$ may be neither mutual nor any other kind of friction can occur until $\mathbf{v}_s$ exceeds $\mathbf{v}_{s,c}$. (2) For $\mathbf{v}_s > \mathbf{v}_{s,c} = \mathbf{v}_{s,c}^*$ in heat flow at low temperatures, $\mathbf{F}_s$, which depends upon $(\mathbf{v}_s - \mathbf{v}_{s,c})$, is completely swamped by the large mutual friction force associated with high relative velocities; it therefore appears that the full value of $\mathbf{F}_{sn}$ is suddenly turned on as $\mathbf{v}_s$ exceeds $\mathbf{v}_{s,c}$, so that in this type of experiment the effects of $\mathbf{F}_s$ are difficult to detect. This statement implies that for heat flow at low temperatures (6) should be rewritten as

$$\left.\begin{aligned} \frac{\rho}{\rho_s}\,\mathbf{F}_{sn} &= A\rho\rho_n(\mathbf{v}_s - \mathbf{v}_n)^3 && \mathbf{v}_s > \mathbf{v}_{s,c} = \mathbf{v}^*_{s,c} \\ &= 0 && \mathbf{v}_s < \mathbf{v}_{s,c} = \mathbf{v}^*_{s,c} \end{aligned}\right\} \qquad (6')$$

(3) For $\mathbf{v}_s > \mathbf{v}_{s,c}$ in isothermal flow the situation is reversed, with $\mathbf{F}_s$ dominating $\mathbf{F}_{s,n}$, since $\mathbf{v}_r$ in such experiments is small.

Now let us see what happens when these different kinds of flow experiments are considered at higher temperatures. The observations show that $\mathbf{v}^*_{s,c}$ becomes larger than $\mathbf{v}_{s,c}$, suggesting that in a heat flow at high temperatures vortices are indeed still formed at $\mathbf{v}_s = \mathbf{v}_{s,c}$ but that $\mathbf{v}_r$ at this point is too small to satisfy the homogeneity conditions for producing a fully developed mutual friction. However at $\mathbf{v}_{s,c}$ superfluid friction must begin and one might also expect to observe some kind of interaction between the vortices that are created and the flowing normal fluid. Evidently these effects are too small to be observed in the heat flow experiments so that $\mathbf{v}_s$ must increase, and also $\mathbf{v}_r$, until at $\mathbf{v}_s = \mathbf{v}^*_{s,c}$ the vortices become sufficiently closely spaced to allow $\mathbf{F}_{sn}$ to be described by (6′). This explanation is reasonable in view of the fact that in the heat flow experiments as T_0 increases, the value of $\mathbf{v}_r$ corresponding to $\mathbf{v}_{s,c}$ decreases rapidly. For Slit III′, with $T_0 = 2.0°\mathrm{K}$, $\mathbf{v}_r$ at $\mathbf{v}_s = \mathbf{v}^*_{s,c}$ has decreased to about 13 cm/sec, almost a factor of ten lower than its value for $T_0 = 1.15°\mathrm{K}$, but $\mathbf{v}_r$ at $\mathbf{v}_s = \mathbf{v}_{s,c}$ is only about 5 cm/sec, not much greater than $\mathbf{v}_{s,c}$ itself and too small to make $\mathscr{L}$ comparable with d. The actual situation is much too complicated to make the argument completely quantitative, but the line of reasoning pursued above does give some indications as to how apparently different critical velocities may arise using different experimental methods even with the same geometry.

Acknowledgment

The authors wish to express their appreciation to Dr. R. Keith Zeigler for assistance with the numerical analysis.

References

1. For reviews on this subject see K.R. ATKINS, *Liquid Helium*, Chapter 6. Cambridge University Press, Cambridge (1959); also V.P. PESHKOV in *Progress in Low Temperature Physics*, (C.J. Gorter, ed.) Vol. IV, p. 1 ff. North Holland, Amsterdam (1964).

2. K.R. ATKINS, *op. cit.*, p. 200.

3. W.E. KELLER and E.F. HAMMEL, *Ann. Phys.* **10**, 202 (1960); E.F. HAMMEL and W.E. KELLER, *Phys. Rev.* **124**, 1641 (1961).

4. W.E. KELLER and E.F. HAMMEL, *Cryogenics* **5**, 245 (1965).

5. E.F. HAMMEL, *Rev. Sci. Instrum.* **36**, 705 (1965).

6. H.C. KRAMERS, private communication.

7. R.P. FEYMAN in *Progress in Low Temperature Physics*, (C.J. Gorter, ed.) Vol. I, p. 17 ff. North Holland, Amsterdam (1955); also W.F. VINEN, *ibid.*, Vol. III, p. 1 ff. (1961).

8. P.P. CRAIG, W.E. KELLER and E.F. HAMMEL, *Ann. Phys.* 21, 72 (1963).

9. H. LAMB, *Hydrodynamics* (6th Ed.) p. 239, Cambridge University Press, Cambridge (1952).

10. V.P. PESHKOV in *Proceedings of VIIth International Conference on Low Temperature Physics*, (G.M. Graham and A.C. Hollis Hallett, eds.), pp. 555-557. University of Toronto Press (1961).

11. V.L. GINZBURG and L.P. PITAEVSKY, *J. exp. theor. Phys.* 34, 1240 (1958); English translation, *Sov. Phys. JETP* 7, 858 (1958).

12. D.F. BREWER and D.O. EDWARDS, *Phil. Mag.* 6, 775 (1961).

13. P.W. ANDERSON, *Sussex University Symposium on Quantum Fluids*, North Holland, Amsterdam.

14. S.T. BELIAEV, *J. exp. theor. Phys.* 34, 417 (1958); English translation, *Sov. Phys. JETP* 7, 289 (1958).

15. V.P. PESHKOV and V.B. STRUKOV, *J. exp. theor. Phys.* 41, 1443 (1961); English translation, *Sov. Phys. JETP* 14, 1031 (1962).

16. W.F. VINEN, *Proc. Roy. Soc.* A242, 493 (1957).